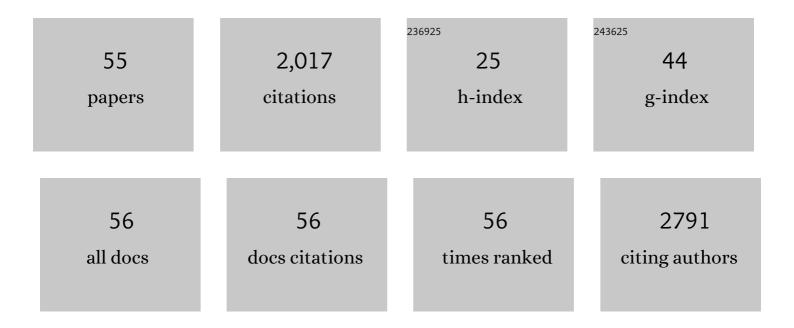
Yu-Hao Li

List of Publications by Year in descending order

Source: https://exaly.com/author-pdf/1027463/publications.pdf Version: 2024-02-01



Υμ-Ηλο Ιι

#	Article	IF	CITATIONS
1	Ultrasensitive Near-Infrared Fluorescence-Enhanced Probe for <i>in Vivo</i> Nitroreductase Imaging. Journal of the American Chemical Society, 2015, 137, 6407-6416.	13.7	408
2	An AlE-active boron-difluoride complex: multi-stimuli-responsive fluorescence and application in data security protection. Chemical Communications, 2014, 50, 12951-12954.	4.1	183
3	A bioprobe based on aggregation induced emission (AIE) for cell membrane tracking. Chemical Communications, 2013, 49, 11335.	4.1	122
4	GSH-activated MRI-guided enhanced photodynamic- and chemo-combination therapy with a MnO ₂ -coated porphyrin metal organic framework. Chemical Communications, 2019, 55, 6241-6244.	4.1	62
5	Effects of Extended Ï€-Conjugation in Phenanthroline (N ^{â^§} N) and Phenylpyridine (C ^{â^§} N) Ligands on the Photophysics and Reverse Saturable Absorption of Cationic Heteroleptic Iridium(III) Complexes. Journal of Physical Chemistry C, 2014, 118, 6372-6384.	3.1	58
6	Targeted imaging and targeted therapy of breast cancer cells <i>via</i> fluorescent double template-imprinted polymer coated silicon nanoparticles by an epitope approach. Nanoscale, 2019, 11, 17018-17030.	5.6	58
7	Ratiometric Monitoring of Intracellular Drug Release by an Upconversion Drug Delivery Nanosystem. ACS Applied Materials & Interfaces, 2015, 7, 12278-12286.	8.0	57
8	Synthesis and adsorption performance of La@ZIF-8 composite metal–organic frameworks. RSC Advances, 2020, 10, 3380-3390.	3.6	56
9	AIE-active Ir(<scp>iii</scp>) complexes with tunable emissions, mechanoluminescence and their application for data security protection. Journal of Materials Chemistry C, 2016, 4, 2553-2559.	5.5	54
10	A cation-exchange controlled core–shell MnS@Bi ₂ S ₃ theranostic platform for multimodal imaging guided radiation therapy with hyperthermia boost. Nanoscale, 2017, 9, 14364-14375.	5.6	53
11	Nonlinear Absorbing Cationic Iridium(III) Complexes Bearing Benzothiazolylfluorene Motif on the Bipyridine (Nâ^§N) Ligand: Synthesis, Photophysics and Reverse Saturable Absorption. ACS Applied Materials & Interfaces, 2013, 5, 6556-6570.	8.0	50
12	Nanozyme-Incorporated Biodegradable Bismuth Mesoporous Radiosensitizer for Tumor Microenvironment-Modulated Hypoxic Tumor Thermoradiotherapy. ACS Applied Materials & Interfaces, 2020, 12, 57768-57781.	8.0	47
13	Influence of Different Diimine (N ^{â^§} N) Ligands on the Photophysics and Reverse Saturable Absorption of Heteroleptic Cationic Iridium(III) Complexes Bearing Cyclometalating 2-{3-[7-(Benzothiazol-2-yl)fluoren-2-yl]phenyl}pyridine (C ^{â^§} N) Ligands. Journal of Physical Chemistry C. 2014. 118. 23233-23246.	3.1	40
14	Biodegradable BiOCl platform for oxidative stress injury–enhanced chemodynamic/radiation therapy of hypoxic tumors. Acta Biomaterialia, 2021, 129, 280-292.	8.3	39
15	Bistratal Au@Bi2S3 nanobones for excellent NIR-triggered/multimodal imaging-guided synergistic therapy for liver cancer. Bioactive Materials, 2021, 6, 386-403.	15.6	38
16	Tumor Microenvironment Modulation Platform Based on Composite Biodegradable Bismuth–Manganese Radiosensitizer for Inhibiting Radioresistant Hypoxic Tumors. Small, 2021, 17, e2101015.	10.0	38
17	Folic acid-nanoscale gadolinium-porphyrin metal-organic frameworks: fluorescence and magnetic resonance dual-modality imaging and photodynamic therapy in hepatocellular carcinoma. International Journal of Nanomedicine, 2019, Volume 14, 57-74.	6.7	35
18	Long-lived platinum(ii) diimine complexes with broadband excited-state absorption: efficient nonlinear absorbing materials. Dalton Transactions, 2012, 41, 12353.	3.3	34

Yu-Hao Li

#	Article	IF	CITATIONS
19	Synthesis, photophysics and reverse saturable absorption of bipyridyl platinum(ii) bis(arylfluorenylacetylide) complexes. Dalton Transactions, 2013, 42, 4398.	3.3	34
20	Ultrafast Synthesizing Bismuth Mesoporous Nanolitchi Radiosensitizer Loading High Dose DOX for CT-Guided Enhanced Chemoradiotherapy. ACS Applied Materials & Interfaces, 2019, 11, 42932-42942.	8.0	34
21	Sorafenib-Conjugated Zinc Phthalocyanine Based Nanocapsule for Trimodal Therapy in an Orthotopic Hepatocellular Carcinoma Xenograft Mouse Model. ACS Applied Materials & Interfaces, 2020, 12, 17193-17206.	8.0	34
22	Ultrasound and Near-Infrared Light Dual-Triggered Upconversion Zeolite-Based Nanocomposite for Hyperthermia-Enhanced Multimodal Melanoma Therapy via a Precise Apoptotic Mechanism. ACS Applied Materials & Interfaces, 2020, 12, 32420-32431.	8.0	32
23	An AIPE-active heteroleptic Ir(III) complex for latent fingermarks detection. Sensors and Actuators B: Chemical, 2018, 259, 840-846.	7.8	30
24	Biodegradable Bismuthâ€Based Nanoâ€Heterojunction for Enhanced Sonodynamic Oncotherapy through Charge Separation Engineering. Advanced Healthcare Materials, 2022, 11, e2102503.	7.6	28
25	Dual-light triggered metabolizable nano-micelles for selective tumor-targeted photodynamic/hyperthermia therapy. Acta Biomaterialia, 2021, 119, 323-336.	8.3	25
26	Mesoporous Bi-Containing Radiosensitizer Loading with DOX to Repolarize Tumor-Associated Macrophages and Elicit Immunogenic Tumor Cell Death to Inhibit Tumor Progression. ACS Applied Materials & Interfaces, 2020, 12, 31225-31234.	8.0	24
27	X-ray and NIR light dual-triggered mesoporous upconversion nanophosphor/Bi heterojunction radiosensitizer for highly efficient tumor ablation. Acta Biomaterialia, 2020, 113, 570-583.	8.3	24
28	Synthesis and photophysics of reverse saturable absorbing heteroleptic iridium(<scp>iii</scp>) complexes bearing 2-(7-R-fluoren-2′-yl)pyridine ligands. Dalton Transactions, 2014, 43, 1724-1735.	3.3	23
29	Regulation of zeolite-derived upconversion photocatalytic system for near infrared light/ultrasound dual-triggered multimodal melanoma therapy under a boosted hypoxia relief tumor microenvironment via autophagy. Chemical Engineering Journal, 2022, 429, 132484.	12.7	21
30	Aza-boron-diquinomethene complexes bearing N-aryl chromophores: synthesis, crystal structures, tunable photophysics, the protonation effect and their application as pH sensors. Journal of Materials Chemistry C, 2015, 3, 3774-3782.	5.5	20
31	Electrostatic self-assembled Iridium(III) nano-photosensitizer for selectively disintegrated and mitochondria targeted photodynamic therapy. Dyes and Pigments, 2020, 175, 108105.	3.7	20
32	Functionalization of bismuth sulfide nanomaterials for their application in cancer theranostics. Chinese Chemical Letters, 2020, 31, 3015-3026.	9.0	20
33	Structural properties and in vitro and in vivo immunomodulatory activity of an arabinofuranan from the fruits of Akebia quinata. Carbohydrate Polymers, 2021, 256, 117521.	10.2	20
34	Ultrafast synthesis of fluorine-18 doped bismuth based upconversion nanophosphors for tri-modal CT/PET/UCL imaging <i>in vivo</i> . Chemical Communications, 2019, 55, 7259-7262.	4.1	18
35	PEGylated iridium-based nano-micelle: Self-assembly, selective tumor fluorescence imaging and photodynamic therapy. Dyes and Pigments, 2020, 182, 108651.	3.7	16
36	An AEE-active probe combined with cyanoacrylate fuming for a high resolution fingermark optical detection. Sensors and Actuators B: Chemical, 2019, 283, 99-106.	7.8	14

Yu-Hao Li

#	Article	IF	CITATIONS
37	Bismuthâ€Based Mesoporous Nanoball Carrying Sorafenib for Computed Tomography Imaging and Synergetic Chemoradiotherapy of Hepatocellular Carcinoma. Advanced Healthcare Materials, 2020, 9, e2000650.	7.6	14
38	BSA-encapsulated cyclometalated iridium complexes as nano-photosensitizers for photodynamic therapy of tumor cells. RSC Advances, 2021, 11, 15323-15331.	3.6	14
39	<p>The Application of Methylprednisolone Nanoscale Zirconium-Porphyrin Metal-Organic Framework (MPS-NPMOF) in the Treatment of Photoreceptor Degeneration</p> . International Journal of Nanomedicine, 2019, Volume 14, 9763-9776.	6.7	13
40	Influence of a Naphthaldiimide Substituent at the Diimine Ligand on the Photophysics and Reverse Saturable Absorption of Pt ^{II} Diimine Complexes and Cationic Ir ^{III} Complexes. European Journal of Inorganic Chemistry, 2015, 2015, 5241-5253.	2.0	11
41	Computed Tomography Imaging-Guided Tandem Catalysis-Enhanced Photodynamic Therapy with Gold Nanoparticle Functional Covalent Organic Polymers. ACS Applied Bio Materials, 2020, 3, 2534-2542.	4.6	11
42	SiO 2 encapsulated nanofluorophor: Photophysical properties, aggregation induced emission and its application for cell mitochondria imaging. Dyes and Pigments, 2017, 139, 110-117.	3.7	10
43	Knockout of zebrafish interleukin 7 receptor (IL7R) by the CRISPR/Cas9 system delays retinal neurodevelopment. Cell Death and Disease, 2018, 9, 273.	6.3	10
44	A biodegradable bismuth–gadolinium-based nano contrast agent for accurate identification and imaging of renal insufficiency <i>in vivo</i> . Inorganic Chemistry Frontiers, 2021, 8, 4720-4729.	6.0	9
45	Intraperitoneal Injection of Cyanine-Based Nanomicelles for Enhanced Near-Infrared Fluorescence Imaging and Surgical Navigation in Abdominal Tumors. ACS Applied Bio Materials, 2021, 4, 5695-5706.	4.6	8
46	Benzothiazole-decorated iridium-based nanophotosensitizers for photodynamic therapy of cancer cells. Dalton Transactions, 2022, 51, 3666-3675.	3.3	7
47	Fluorescent Imaging-Guided Chemo- and Photodynamic Therapy of Hepatocellular Carcinoma with HCPT@NMOFs-RGD Nanocomposites. International Journal of Nanomedicine, 2022, Volume 17, 1381-1395.	6.7	7
48	Knockout of zebrafish colony-stimulating factor 1 receptor by CRISPR/Cas9 affects metabolism and locomotion capacity. Biochemical and Biophysical Research Communications, 2021, 551, 93-99.	2.1	6
49	Lanthanide-doped bismuth-based nanophosphors for ratiometric upconversion optical thermometry. RSC Advances, 2022, 12, 8743-8749.	3.6	6
50	Quantitative hypoxia mapping using a self-calibrated activatable nanoprobe. Journal of Nanobiotechnology, 2022, 20, 142.	9.1	6
51	<p>Celecoxib Exerts a Therapeutic Effect Against Demyelination by Improving the Immune and Inflammatory Microenvironments</p> . Journal of Inflammation Research, 2020, Volume 13, 1043-1055.	3.5	5
52	Rapid electrochemical detection of MiRNA-21 facilitated by the excellent catalytic ability of Pt@CeO ₂ nanospheres. RSC Advances, 2022, 12, 11867-11876.	3.6	5
53	How Do Bismuth-Based Nanomaterials Function as Promising Theranostic Agents for the Tumor Diagnosis and Therapy?. Current Medicinal Chemistry, 2022, 29, 1866-1890.	2.4	2
54	Ultrasound-triggered reactive oxygen species effector nanoamplifier for enhanced combination therapy of mutant p53 tumors. Colloids and Surfaces B: Biointerfaces, 2022, 215, 112489.	5.0	2

#	Article	IF	CITATIONS
55	Near-Infrared Frequency Upconversion Luminescence Bioimaging Based on Cyanine Nanomicelles. ACS Applied Polymer Materials, 2022, 4, 5566-5573.	4.4	2